ELSEVIER

Available online at www.sciencedirect.com
SCIENCE DIRECT®

Applied Surface Science 252 (2006) 3532–3540

applied surface science

www.elsevier.com/locate/apsusc

# Self-assembled monolayer growth on chemically modified polymer surfaces

S. Pimanpang *, Pei-I. Wang, G.-C. Wang, T.-M. Lu

*Department of Physics, Applied Physics, and Astronomy, and Center for Integrated Electronics, Rensselaer Polytechnic Institute, Troy, NY 12180-3590, USA*

Received 9 January 2005; accepted 16 May 2005
Available online 11 July 2005

**Abstract**

We report a study of the self-assembled monolayer (SAM) growth of bis[3(triethoxysilane)propyl]tetrasulfide (Tetrasulfide) on low dielectric constant (low-*k*) aromatic hydrocarbon SiLK whose surface chemistry was modified using sulfuric acid, He plasma treatment, and $N_2$ plasma treatment. X-ray photoelectron spectroscopy (XPS) spectra show that there is no detectable growth of Tetrasulfide SAM on untreated SiLK surfaces. After the SiLK surfaces have been treated with sulfuric acid, He plasma, or $N_2$ plasma, the original chemically inert polymer surfaces are functionalized with polar groups resulting in a significant improvement of their wettability, which is confirmed by their reduction of water droplet contact angles. The introduction of polar functional groups thus facilitates the formation of Tetrasulfide SAM on the polymer surfaces. Atomic force microscopy (AFM) analysis shows an insignificant change in the surface morphology after the growth of Tetrasulfide SAM on the chemically modified SiLK surfaces. Quantitative XPS analysis also showed that Tetrasulfide SAM growth is more prominent on He and $N_2$ plasma treated surfaces than those treated by sulfuric acid.
© 2005 Elsevier B.V. All rights reserved.

*Keywords:* SiLK; Self-assembled monolayer; Plasma treatment; AFM; XPS; Contact angle

## 1. Introduction

As the scale of microelectronic devices continues to shrink, interconnect delay increasingly dominates the performance of integrated circuits (ICs). The implementations of integrating Cu as the conductor with low-*k* dielectrics can effectively reduce the interconnect delay. A variety of low-*k* candidates have emerged to meet the dielectric requirements [1–3]. Recently, an aromatic hydrocarbon polymer, SiLK, which has a low dielectric constant and inherently can resist moisture uptake, has been receiving attention in semiconductor industry [1].

However, SiLK, as most of the polymers, generally has poor adhesion properties to metals due to its chemically inert nature. Various techniques have been adopted to improve metal adhesion to the polymer surfaces, such as ion bombardment, plasma treatment,

* Corresponding author. Tel.: +1 518 276 8387;
fax: +1 518 276 6680.
*E-mail address:* pimans@rpi.edu (S. Pimanpang).

0169-4332/$ – see front matter © 2005 Elsevier B.V. All rights reserved.
doi:10.1016/j.apsusc.2005.05.049

and acid treatments [4–7]. In some instances, one would roughen the polymer surfaces in order to form a mechanical interlock at the metal–polymer interface [8]. Chemical modification of the native polymer surfaces can be achieved by introducing functional groups onto the polymer surfaces, such as –SH or –OH, to activate the polymer surfaces for metallization. It is known that Cu–O interaction is weak resulting in poor Cu wetting, but Cu–S interaction is strong, which will allow Cu to wet sulfide surface [9,10]. Thus, the introduction of S onto the polymer surface is a promising approach to achieve Cu wetting and adhesion on a SiLK surface.

Self-assembled monolayer (SAM) technique allows one to grow thin organic films uniformly on solid surfaces. SAM can serve as a passivation layer and can modify surface properties [9,11–21]. Mercaptan and Tetrasulfide SAMs have been studied and they can be formed on hydroxylated $SiO_2$ surface resulting in the improvement of Cu adhesion and wettability to the $SiO_2$ surface. Tetrasulfide is more stable against oxidation in ambient than Mercaptan because it has a tetrasulfide chemical moiety (–SSSS–) as opposed to the Mercaptan moiety (–SH) [9]. To provide a wettable SiLK surface for Tetrasulfide SAM growth, polar functional groups, such as hydroxyl bonds (–OH), have to be introduced through proper surface treatments to modify the originally hydrophobic SiLK surface.

In this study, we investigate the characteristics of Tetrasulfide SAM growth on both acid treated and plasma treated SiLK surfaces. Either He or $N_2$ plasma was utilized to modify the SiLK surface. The surface morphology of SiLK polymer before and after the Tetrasulfide SAM growth is characterized using atomic force microscopy (AFM), and the surface chemistry is characterized using X-ray photoelectron spectroscopy (XPS).

## 2. Experiment

### 2.1. Sample preparation

SiLK polymer films were spin-coated onto Si wafers. The $H_2SO_4$ solution (50 vol.%) was used as the acid surface treatment at room temperature. SiLK-coated samples were dipped into the $H_2SO_4$ solution for 30 s and then rinsed by deionized water (DI water). The samples were dried by nitrogen blow dry and then baked out at 100 °C for 30 min in $N_2$ environment. The He and $N_2$ plasma treatments were conducted at a power of 100 W, a gas pressure of 0.5 Torr, and a gas flow rate at 400 sccm for 1 min.

We prepared two sets of samples for the growth of Tetrasulfide SAM on untreated SiLK, SiLK treated with sulfuric acid, He plasma, and $N_2$ plasma. One set was for AFM and contact angle measurements, and the other set for the XPS measurement. A solution mixed with 7 mg of bis[3(triethoxysilane)propyl]tetrasulfide (Tetrasulfide) per gram of toluene was prepared at room temperature. Each sample was dipped into the solution for 40 min. The samples were rinsed with toluene four times and dried by nitrogen blow dry. After the Tetrasulfide SAM growth, the XPS sample set was loaded into the XPS chamber immediately.

### 2.2. Contact angle measurements

In the contact angle measurements, a 2 μL distilled water in a syringe was dropped on the sample surface at room temperature. It is also called the sessile drop technique [22]. The water droplet formed an equilibrium dome shape on the sample surface and was imaged by an optical microscope with 60 times magnification. The contact angle of the water droplet was analyzed using a computer software developed in-house.

### 2.3. AFM and XPS measurements

The surface structures were imaged by AFM and analyzed using the associated image software (Park Scientific Instrument). Surface images were obtained using the non-contact mode at three different places on each sample to get an average surface morphology. The surface chemical bonding on each sample was analyzed using XPS. The samples were loaded into a stainless chamber with a base pressure range of 2–$4 \times 10^{-9}$ Torr. During the collection of an XPS spectrum, the pressure raised to the range of 4–$6 \times 10^{-9}$ Torr. The X-ray Mg Kα source (*PHI model 04-151*) used in this experiment had a primary energy of 1253.6 eV, and a double pass cylindrical mirror energy analyzer (*PHI Model 15-255G*) was used to detect the electrons. The X-ray source was operated at

~270 W with 10 kV high voltage bias and 27 mA emission current. An average high-resolution spectrum was collected at a passing energy of 50 eV with 40 repeated scans.

## 3. Results and discussions

### 3.1. Acid and plasma treated SiLK surfaces

Table 1 shows the experimental results of the water droplet contact angle measurements on SiLK surfaces before and after treated with sulfuric acid, He plasma, or $N_2$ plasma. The contact angle decreases significantly from ~72° of the originally as-deposited SiLK surface to ~35°, ~33°, and ~5°, for sulfuric acid, He plasma, and $N_2$ plasma treated surfaces, respectively. The decrease of the water droplet contact angle suggests that the polymer surfaces have been transformed from hydrophobic to hydrophilic after these surface treatments. However, the corresponding root mean square roughness (rms) obtained from the AFM analyses shows that the surface morphology of SiLK, SiLK treated with sulfuric acid, and plasmas appears to have no significant changes. These measured rms roughness of untreated SiLK, SiLK treated with sulfuric acid, He plasma, and $N_2$ plasma are $0.66 \pm 0.09$, $0.80 \pm 0.30$, $0.69 \pm 0.05$, and $0.69 \pm 0.07$ nm, respectively.

The water droplet contact angle depends on both the surface morphology and surface chemistry [23]. The change of either the surface morphology or surface chemistry of a giving surface would modify its surface energy leading to the change in the water droplet contact angle. The fact that the SiLK surface morphology, after the sulfuric acid and plasma treatments, showed very little change in the rms roughness suggests that the reduction of the water droplet contact angle is mainly attributed to the functionalization of the polymer surfaces [24].

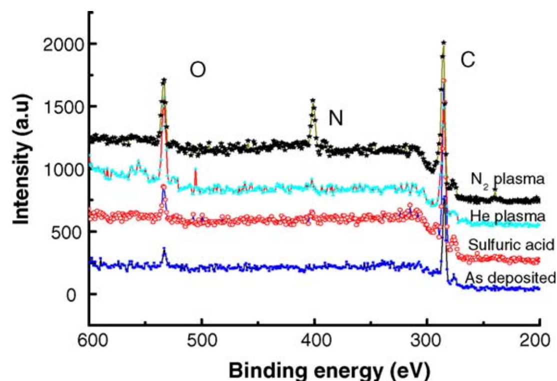


Fig. 1. The XPS spectra of untreated SiLK and SiLK treated with sulfuric acid, He plasma, and $N_2$ plasma. The SiLK treated with sulfuric acid and He plasma show the increase in oxygen peak, but SiLK treated with $N_2$ plasma shows the increase in both oxygen and nitrogen peaks.

The XPS spectrum of the untreated SiLK surface is shown in Fig. 1. The spectrum indicates that SiLK mainly contains carbon and a small amount of oxygen. The SiLK structure and its cross-link are shown in Fig. 2a. The small amount of oxygen seen from the XPS spectrum of the as-deposited SiLK surface may come from the contamination on the surface. The SiLK formation is discussed in detail in Ref. [1]. The XPS spectra of SiLK in Fig. 1 show that the oxygen peak intensity increases after being treated with sulfuric acid or plasmas. It is also observed that the oxygen peak intensity of the SiLK sample treated with He plasma increases more than that of the sample treated with sulfuric acid. In the case of SiLK treated with $N_2$ plasma, the increase of both oxygen and nitrogen functional groups is observed. Identification

Table 1
The water droplet contact angle and the AFM root mean square (rms) roughness on untreated SiLK surface and treated SiLK surfaces (sulfuric acid, He plasma, and $N_2$ plasma) before and after Tetrasulfide SAM growth

| Sample | Before Tetrasulfide SAM growth | | After Tetrasulfide SAM growth | |
|---|---|---|---|---|
| | Contact angle (±2°) | Root mean square roughness (nm) | Contact angle (±2°) | Root mean square roughness (nm) |
| SiLK untreated | 72 | $0.66 \pm 0.09$ | 70 | $1.20 \pm 0.04$ |
| SiLK treated with sulfuric acid | 35 | $0.80 \pm 0.30$ | 53 | $1.00 \pm 0.23$ |
| SiLK treated with He plasma | 33 | $0.69 \pm 0.05$ | 68 | $0.75 \pm 0.03$ |
| SiLK treated with $N_2$ plasma | 5 | $0.69 \pm 0.07$ | 33 | $0.90 \pm 0.02$ |

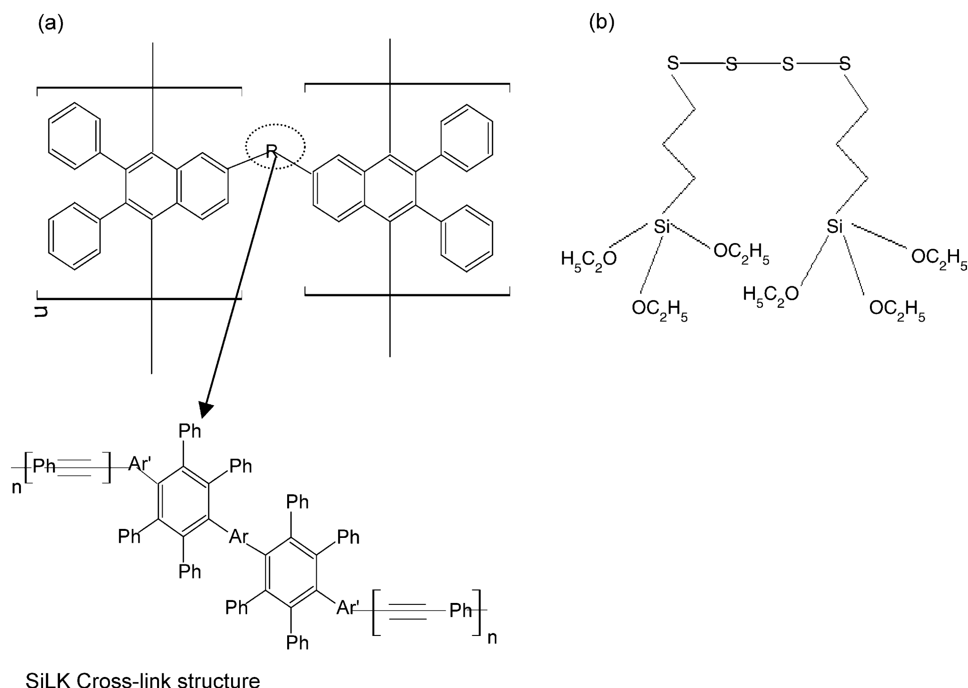


Fig. 2. (a) A schematic of the cross-linked SiLK structure and (b) the bis[3(triethoxysilane)propyl]tetrasulfide (Tetrasulfide) structure.

of those functional groups generated by different surface treatments can be obtained through the decomposition of the XPS C 1s spectra.

Fig. 3a shows that the C 1s spectrum of the as-deposited SiLK is decomposed into two components: C–C (C1) and C–O (C2) at the binding energies of 285.0 and 286.4 eV, respectively. The surface charging effect has been removed by referencing to the C–C peak at 285 eV. The SiLK $\pi$–$\pi^*$ shakeup satellite peak is at 292.5 eV, which is associated with the aromatic ring in the polymer. After SiLK has been treated with sulfuric acid, the C 1s spectrum can be decomposed into three components: C–C (C1), C–O (C2), and C=O (C3) with the C=O binding energy of 287.6 eV (as shown in Fig. 3b). The increase of the C–O bonding percentage compared to that of as-deposited SiLK and the existence of the C=O bonding after it has been treated with sulfuric acid is because the carbon–carbon triple bonds in the cross-linked polymer react with the sulfuric acid solution, resulting in the formation of the oxygen functional groups (–OH and =O) on the surface [24].

The surface modification by He plasma is different from that by acid treatment. He plasma treatment can introduce free radicals onto the SiLK surface. The free radicals have high affinity to oxygen when exposed to air, resulting in the formation of the oxygen functional groups on the surface. This reaction is somewhat more aggressive than that of the acid treatment and leads to the higher oxygen peak intensity shown in Fig. 1. The C 1s spectrum of SiLK treated with He plasma can be decomposed into four components: C–C (C1), C–O (C2), C=O (C3), and O=C–O (C4), with O=C–O binding energy is 289.6 eV as shown in Fig. 3c. A similar situation has been observed on Ar plasma treated SiLK surface. The Ar plasma treatment introduced free radicals that react with oxygen in air leading to the formation of the oxygen functional groups (–O–O– and –OH) on the SiLK surface [18,19].

In the case of $N_2$ plasma treatment, the $N_2$ plasma not only introduces free radicals onto the SiLK surface, but also reacts with the polymer surface to form the nitrogen functional groups. Fig. 1 shows that SiLK surface, after the $N_2$ plasma treatment and an

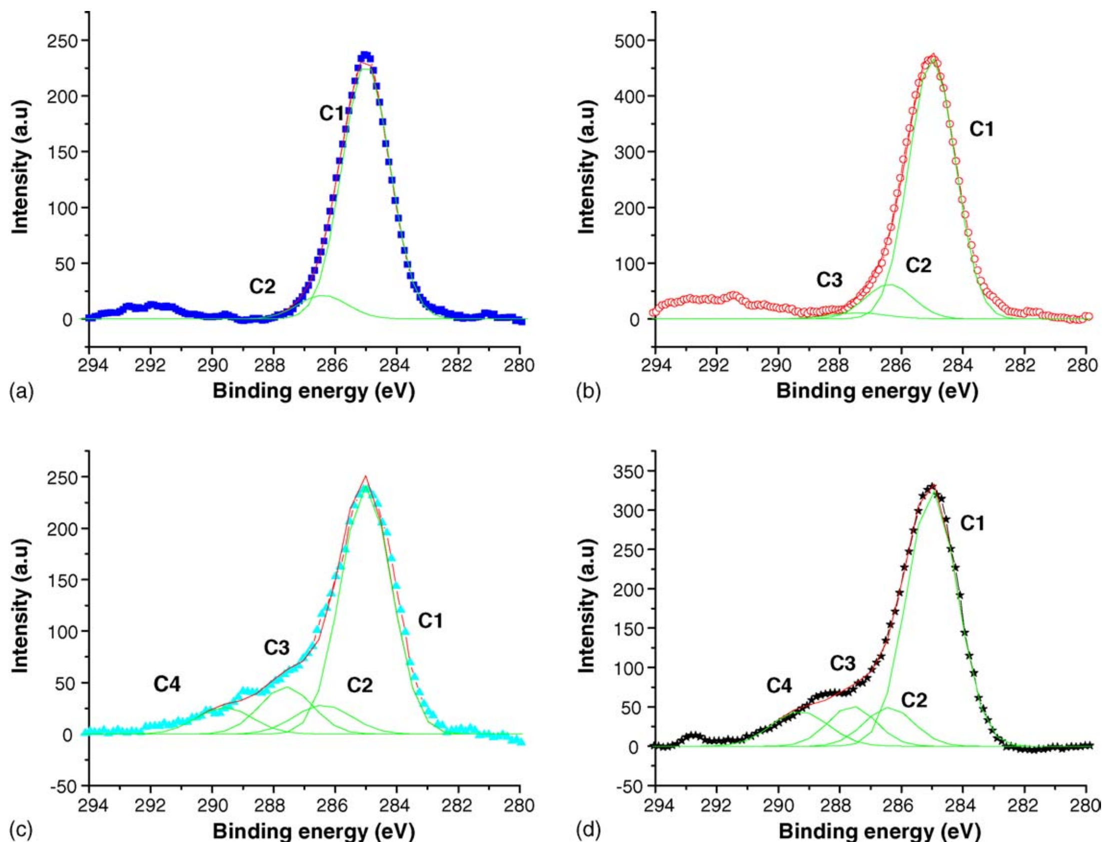


Fig. 3. The C 1s peak of (a) untreated SiLK surface, (b) SiLK surface treated with sulfuric acid, (c) SiLK surface treated with He plasma, and (d) SiLK surface treated with $N_2$ plasma. The C1, C2, C3, and C4 are C–C, C–O, C═O, and O–C═O, respectively.

exposure to ambient, contains both oxygen and nitrogen functional groups. The C 1s spectrum of SiLK treated with $N_2$ plasma can be decomposed into four components as shown in Fig. 3d: C–C (C1), C–O (C2), C═O (C3), and O═C–O (C4). Since the binding energy of the amine (C–$NH_2$) is about 285.8 eV and the binding energy of imine (C═NH) is about 287 eV, which are difficult to resolve from the binding energies of C–O and C═O, so we do not attempt to decompose them. The detail of the nitrogen functional groups formed on SiLK surface is thus identified through the decomposition of the XPS N 1s spectrum.

The XPS N 1s spectrum of SiLK surface treated with $N_2$ plasma can be decomposed into three components: C–$NH_2$ (N1), C═NH (N2), and C–NHOH (N3) as shown in Fig. 4. We observed that the imine group (N2) has the highest percentage of ~71%

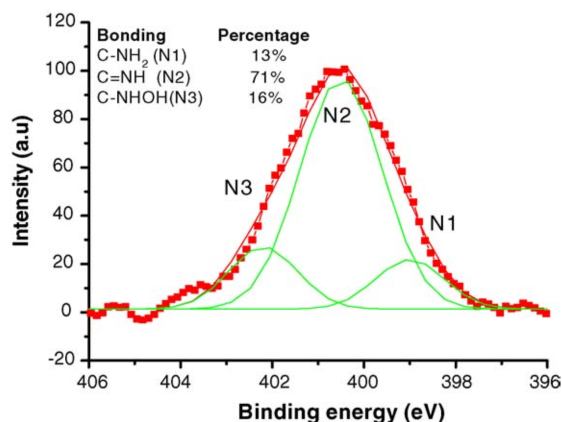


Fig. 4. The N 1s peak of SiLK surface treated with $N_2$ plasma which can be decomposed into C═NH (N1), C–$NH_2$ (N2), and C–NHOH (N3) components.

on the SiLK surface, and N1 and N3 are about 13% and 16%, respectively. Similar results have been reported on $N_2$ plasma treated polystyrene and polypropylene surfaces [25,26]. The nitrogen functional groups significantly improve SiLK wettability as the water droplet contact angle decreases dramatically from $\sim 72^{\circ}$ to $\sim 5^{\circ}$. The water droplet contact angle on SiLK treated with $N_2$ plasma sample is the lowest compared to those of sulfuric acid and He plasma treated samples. This suggests that SiLK treated with $N_2$ plasma surface has the highest surface energy.

### 3.2. Tetrasulfide SAM growth

The chemical reaction between Tetrasulfide and SiLK surfaces was analyzed by XPS. Fig. 2b shows the Tetrasulfide structure which contains a tetrasulfide chemical moiety (–SSSS–). Fig. 5 shows no sign of the S 1s peak after attempting to grow Tetrasulfide on the untreated SiLK. This indicates that Tetrasulfide cannot grow on the originally hydrophobic SiLK surface. However, a sulfur peak in the XPS S 1s spectrum can be observed on Tetrasulfide SAM grown on the SiLK treated surfaces suggesting an improvement of the SiLK surface wettability after being treated with sulfuric acid or plasma. The S 1s spectrum has a main peak at 164.2 eV, which is due to the –SS– bonding. The shoulders on the left side (higher binding energy) of the S 1s peaks are due to the Si plasmon loss (at 168.7 eV) [9]. The S 1s peaks intensity of Tetrasulfide SAM grown on SiLK treated with He plasma or $N_2$ plasma is higher than that of grown on SiLK treated with sulfuric acid, which indicates a higher Tetrasulfide SAM density on SiLK treated with He plasma or $N_2$ plasma. A possible reason that causes the different Tetrasulfide SAM density is due to the higher amount of functional groups introduced by the $N_2$ plasma or He plasma treatment than by the sulfuric acid treatment as shown in Fig. 3.

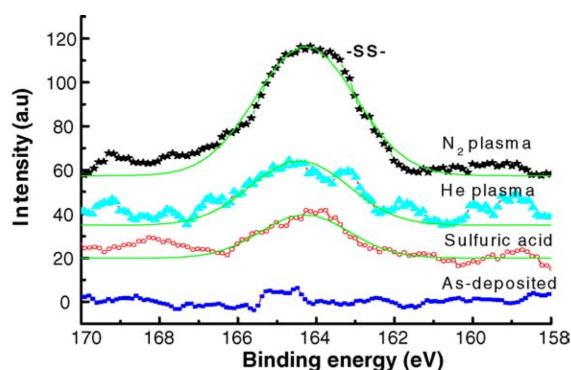


Fig. 5. The S 1s peak of Tetrasulfide SAM grown on untreated SiLK surface and SiLK surfaces treated with sulfuric acid, He plasma, and $N_2$ plasma.

The water droplet contact angle is sensitive to the top 1 nm surface, so it is a quick way to detect whether there is any Tetrasulfide SAM grown on the SiLK surface. If Tetrasulfide SAM is formed on the SiLK surface, then the water droplet contact angle will be different because the polar functional group, tetrasulfide moiety (–SSSS–), has a different surface energy. Table 1 shows that the water droplet contact angle on Tetrasulfide SAM growth on untreated SiLK remains unchanged. On the contrary, the water droplet contact angles on Tetrasulfide SAM growth on treated SiLK surfaces show significant increases in the range of about 20–30°. This is due to the change in the surface energy after the Tetrasulfide SAM is formed on the treated SiLK surfaces.

The rms roughness of Tetrasulfide SAM grown on untreated SiLK, SiLK treated with sulfuric acid, He plasma, and $N_2$ plasma are $1.20 \pm 0.04$, $1.00 \pm 0.23$, $0.75 \pm 0.03$, and $0.90 \pm 0.02$ nm, respectively, as listed in Table 1. The AFM results show that the SiLK surface morphology after the Tetrasulfide SAM growth does not undergo a significant change which suggests that the SAM grown on the treated SiLK surfaces maybe conformal.

A better understanding of the chemical reaction between Tetrasulfide and SiLK surface can be obtained through the analysis of the C 1s spectra. The C 1s spectrum of Tetrasulfide SAM grown on the untreated SiLK surface (Fig. 6a) is composed of two components, C–C (C1) and C–O (C2), which are the same as before the Tetrasulfide SAM growth (Fig. 3a). The percentage of the integrated area of the C–C bonding of the untreated SiLK is 91% for both before and after the Tetrasulfide SAM growth (see Table 2). The $\pi$–$\pi^*$ shakeup satellite peak in the C 1s spectrum is still observed after the SAM growth, which indicates that no Tetrasulfide SAM was formed to cover the SiLK aromatic ring.

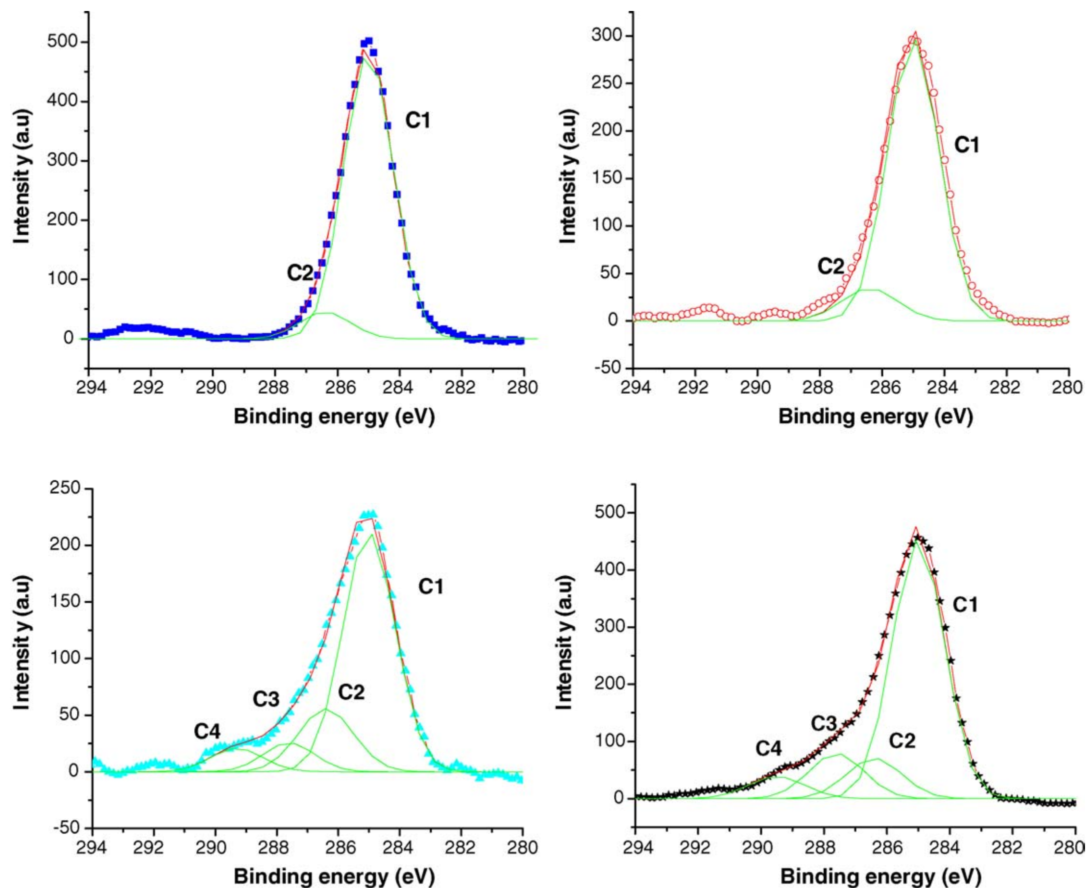


Fig. 6. The C 1s spectra of the Tetrasulfide SAM grown on (a) untreated SiLK surface, (b) SiLK surface treated with sulfuric acid, (c) SiLK surface treated with He plasma, and (d) SiLK surface treated with $N_2$ plasma. The C1, C2, C3, and C4 are C–C, C–O, C═O, and O–C═O, respectively.

However, the change in the C 1s spectra is more significant on Tetrasulfide SAM grown on chemically treated SiLK surfaces than the untreated SiLK surface. It has been reported that the ethoxysilane group ($Si–OC_2H_5$) of the Tetrasulfide can react with hydroxylated $SiO_2$ surface to form Si–O–Si [9]. Since SiLK treated with sulfuric acid is composed of C–OH and C═O groups so one of the possible chemical

Table 2
The percentage of each chemical bond in the C 1s spectra after the decomposition and curve fitting before and after the Tetrasulfide SAM growth on untreated SiLK and treated (sulfuric, He plasma, and $N_2$ plasma) SiLK surfaces

| Sample | Before Tetrasulfide SAMs growth | | | | After Tetrasulfide SAMs growth | | | |
|---|---|---|---|---|---|---|---|---|
| | C–C, 285.0 eV | C–O, 286.4 eV | C═O, 287.6 eV | O═C–O, 289.6 eV | C–C, 285.0 eV | C–O, 286.4 eV | C═O, 287.6 eV | O═C–O, 289.6 eV |
| SiLK untreated | 91 | 9 | – | – | 91 | 9 | – | – |
| SiLK treated with sulfuric acid | 86 | 12 | 2 | – | 89 | 11 | – | – |
| SiLK treated with He plasma | 69 | 9 | 14 | 8 | 67 | 19 | 8 | 6 |
| SiLK treated with $N_2$ plasma | 69 | 10 | 10 | 11 | 69 | 12 | 13 | 6 |

reactions, which can occur between Tetrasulfide and sulfuric acid treated SiLK is:

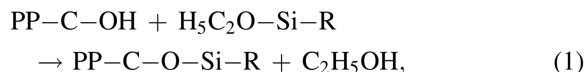

$$\mathrm{PP{-}C{-}OH} + \mathrm{H_5C_2O{-}Si{-}R} \rightarrow \mathrm{PP{-}C{-}O{-}Si{-}R} + \mathrm{C_2H_5OH}, \quad (1)$$

where PP is the SiLK polymer chain, and R is an alkyl of the Tetrasulfide. The C 1s spectrum of Tetrasulfide SAM grown on SiLK treated with sulfuric acid can be decomposed into only two components (C–C and C–O) (Fig. 6b). The C=O component and the $\pi$–$\pi^*$ shakeup satellite peak are not observed because the SiLK surface is covered by the SAM. However, the percentage of C–O bonding after the Tetrasulfide SAM growth is about 11%, which is about the same as that before the Tetrasulfide SAM growth. The absence of a change in the C–O bonding percentage may mainly be attributed to the incomplete hydrolysis of the Tetrasulfide ethoxysilane groups (Si–$OC_2H_5$).

In the case of SiLK treated with He plasma, the surface contains three oxygen functional groups: C–OH, C=O, and COOH. In addition to the aforementioned chemical reaction of Tetrasulfide with C–OH (1), another possibility is the reaction between the Tetrasulfide with COOH on He plasma treated SiLK surface:

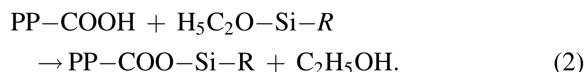

$$\mathrm{PP{-}COOH} + \mathrm{H_5C_2O{-}Si{-}}R \rightarrow \mathrm{PP{-}COO{-}Si{-}R} + \mathrm{C_2H_5OH}. \quad (2)$$

The C 1s spectrum of Tetrasulfide SAM grown on He plasma treated SiLK can be decomposed into four components: C–C, C–O, C=O, and COOH as shown in Fig. 6c. The percentage of the integrated areas of the C=O and COOH peaks decreases, but the percentage of the integrated area of C–O peak increased as listed in Table 2. The decrease of the percentage of C=O and COOH bonds is because the SiLK surface is covered with Tetrasulfide SAM, but the increase of the C–O bonding percentage is possibly due to an incomplete hydrolysis of the Tetrasulfide ethoxysilane group (Si–$OC_2H_5$).

$N_2$ plasma treatment introduces both oxygen and nitrogen functional groups in the SiLK surface. The chemical reaction between Tetrasulfide and oxygen functional group can facilitate SAM growth through both chemical reactions (1) and (2). Besides the reaction of Tetrasulfide with oxygen functional groups, it is also possible to form SAM through the reaction with nitrogen functional groups.

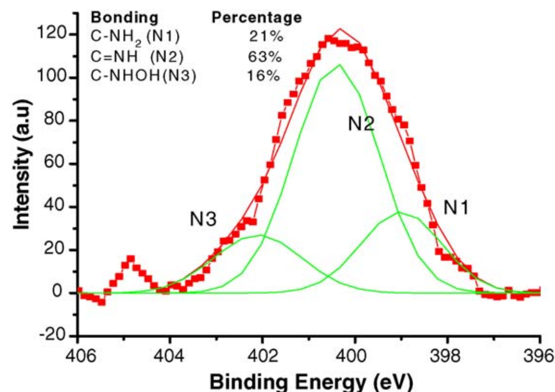


Fig. 7. The N 1s spectra of Tetrasulfide SAM grown on SiLK surface treated with $N_2$ plasma which can be decomposed into three components: C–$NH_2$ (N1), C=NH (N2), and C–NHOH (N3).

Further details of the reaction between Tetrasulfide and nitrogen functional groups are revealed by the change of the N 1s spectrum after the SAM growth. It is observed in Fig. 7 that the imine (C=NH) percentage decreases from 71% (before the SAM growth) to 63%, meanwhile the amine (C–$NH_2$) percentage increases from 13% before the SAM growth to 21% after SAM growth on nitrogen plasma treated SiLK surface. The C–NHOH percentage remains about the same as 16% before and after the SAM growth. The reduction of the imine percentage may be due to the reaction of imine with Tetrasulfide ethoxysilane group (Si–$OC_2H_5$) and/or that imine is hydrolysized with $H_2O$ [27]. Since Tetrasulfide SAM can be possibly formed through the reaction with both oxygen and nitrogen functional groups so that the SAM density on $N_2$ plasma treated SiLK should be higher than those treated with sulfuric acid and He plasma. This suggestion is confirmed by a higher S peak intensity observed in Tetrasulfide SAM grown on $N_2$ plasma treated SiLK surface than those treated with sulfuric acid or He plasma as shown in Fig. 5.

## 4. Conclusions

The growth behavior of Tetrasulfide SAM on low-*k* aromatic hydrocarbon SiLK whose surface chemistry was modified using sulfuric acid, and He and $N_2$ plasma treatments has been studied. It is observed that

the Tetrasulfide cannot grow on the hydrophobic SiLK surface due to the lack of functional groups on the surface. The improvement of SiLK surface wettability through sulfuric acid, He plasma, and $N_2$ plasma treatments significantly increases the efficiency of Tetrasulfide SAM growth on the surface. AFM results show that the change of the surface morphology is not significant after the Tetrasulfide SAM growth on treated SiLK surfaces, which suggests that Tetrasulfide SAM may form a conformal layer on these treated polymer surfaces. XPS provides quantitative analyses on the bonding characteristics of the chemically modified SiLK surfaces. XPS also reveals that the Tetrasulfide SAM growth depends not only on the total amount of polar functional groups created by the surface treatments, but also on the inherent reactivity of each functional group (C–OH, C=O, COOH, C–$NH_2$, C=NH, and C–NHOH) to the Tetrasulfide.

## Acknowledgments

We would like to thank Xiaoping Ao for valuable discussions in chemistry. Samuk Pimanpang would like to thank Thai government fellowship.

## References


[1] S.J. Marting, J.P. Godschalx, M.E. Mills, E.O. Shaffer II, P.H. Townsend, Adv. Mater. 12 (2000) 1769.

[2] J.J. Senkevich, C.J. Mitchell, A. Vijayaraghavan, E.V. Barnat, J.F. McDonald, T.-M. Lu, J. Vac. Sci. Technol. A 20 (2002) 1445.

[3] K.C. Chan, M. Teo, Z.W. Zhong, Microelectron. Int. 20/3 (2003) 11.

[4] B.A. Ratchev, G.S. Was, J.H. Booske, Nucl. Instrum. Methods B 68–73 (1995) 106.

[5] J.J. Senkevich, G.R. Yang, T.M. Lu, Colloids Surf. A 214 (2003) 119.

[6] J.P. Badey, E. Espuche, D. Sage, B. Chabert, Y. Jugnet, C. Batier, T.-M. Duc, Polymer 37 (1996) 1377.

[7] J.F. Friedrich, Sh. Geng, W. Unger, A. Lippitz, J. Erdmann, H.V. Gorsler, Ch. Woll, A. Schertel, K. Bierbaum, Surf. Coat. Technol. 74–75 (1995) 664.

[8] P.K. Wu, T.-M. Lu, Chemical structure determination, modeling, and adhesion enhancement of metal/polymer interfaces, in: K.L. Metal (Ed.), Metallized Plastics 7: Fundamental and Applied Aspects, VSP, Utrecht, 2001, p. 215.

[9] J.-J. Senkevich, B. Li, G.-R. Yang, G.-C. Wang, T.-M. Lu, Electrochem. Solid State Lett. 5 (2002) C94.

[10] L. Chen, N. Magtoto, B. Ekstrom, J. Kelber, Thin Solid Films 376 (2000) 115.

[11] G. Ramanath, G. Cui, P.G. Ganesan, X. Guo, A.V. Ellis, M. Stukowski, K. Vijayamohanan, P. Doppelt, M. Lane, Appl. Phys. Lett. 83 (2003) 383.

[12] M. Hu, S. Noda, Y. Tsuji, T. Okubo, Y. Yamaguchi, H. Komiyama, J. Vac. Sci. Technol. A 20 (2002) 589.

[13] J.J. Senkevich, C.J. Mitchell, G.-R. Yang, T.-M. Lu, Langmuir 18 (2002) 1587.

[14] R. Cueff, G. Baud, M. Benmalek, J.P. Besse, J.R. Butruille, M. Jacquet, Appl. Surf. Sci. 115 (1997) 292.

[15] M.C. Gerstenberg, F. Schreiber, T.Y.B. Leung, G. Bracco, S.R. Forrest, G. Scoles, Phys. Rev. B 61 (2000) 7678.

[16] S. Raible, J. Pfeiffer, T. Weiss, W. Clauss, W. Goepel, V. Schurig, D.P. Kern, Appl. Phys. A 70 (2000) 607.

[17] F. Sun, D.W. Grainger, D.G. Castner, J. Vac. Sci. Technol. A 12 (1994) 2499.

[18] W.H. Yu, Y. Zhang, E.T. Kang, K.G. Neoh, S.Y. Wu, Y.F. Chow, J. Electrochem. Soc. 149 (2002) C521.

[19] W.H. Yu, Y. Zhang, E.T. Kang, K.G. Neoh, S.Y. Wu, Y.F. Chow, J. Electrochem. Soc. 150 (2003) F156.

[20] M.K. Chaudhury, M.J. Owen, J. Phys. Chem. 97 (1993) 5722.

[21] R.N. Mason, M. Smith, T. Andrews, D. Teeters, Solid State Ionics 118 (1999) 129.

[22] I.-D. Morrison, S. Ross, Colloidal Dispersions Suspensions, Emulsion and Foams, John Wiley and Sons, 2002, p. 202.

[23] N. Eustathopoulos, M.G. Nicholas, B. Drevet, Wettability at High Temperatures, Pergamon, 1999, p. 22.

[24] S. Pimanpang, Pei-I. Wang, J.J. Senkevich, G.-C. Wang, T.-M. Lu, Colloids Surf. A, submitted for publication.

[25] B. Mutel, J. Grimblot, O. Dessaux, P. Goudmand, Surf. Interface Anal. 30 (2000) 401.

[26] S.B. Idage, S. Badrinarayanan, Langmuir 14 (1998) 2780.

[27] M. Strobel, C. Lyons, K.L. Mittal, Plasma Surf. Modif. Polym. (1994) 61.